Soils and Rocks
www.soilsandrocks.com
An International Journal of Geotechnical and Geoenvironmental Engineering
ISSN 1980-9743
ISSN-e 2675-5475

Improving mechanical strength and leachability behavior of bauxite tailings for dry stacking using Portland Cement

Gilson Gabriel Teixeira Varela[1], David Braga Fernandes[2], Aldenora Vieira Santos Neta[3], Alisson do Nascimento Lima[4], Lara Pereira Tavares Mendes[2], Manoel Leandro Araújo e Farias[1], Carina Silvani[1#]

Article

Keywords
Mining tailings
Dry stacking
Porosity/volumetric cement content index
Leachability and solubilization analysis

Abstract

The disposal of tailings has become a challenge for the mining sector, environmental agencies, and society. This research aims to analyze the geomechanical and environmental behavior of cemented bauxite tailings (BT) for use in cemented dry tailings piles, a new trend for tailing disposal. The experimental program consisted of a series of unconfined compression tests and splitting tensile tests in BT with addition of 2%, 4%, and 6% of Portland Cement (C_i), and compacted at 18 kN/m³, 19 kN/m³, and 20 kN/m³. Leachability and solubilization tests were done with specimens with 20 kN/m³ and C_i of 0%, 4%, and 6%. All samples were done with water content of 18% and cured for 7 days. Increasing in Portland cement content and dry units of weight increases unconfined compressive strength (q_u) and splitting tensile strength (q_t); therefore, the increase in porosity decreases these mechanical properties. The importance of those parameters was confirmed by ANOVA and Tukey test analysis. The porosity/Portland cement content index allowed the prediction of q_u and q_t of BT-Portland cement blends; however, the q_t/q_u remained constant (0.14) and independent of this index. The environmental analysis showed that the addition of Portland cement to BT reduced the concentration of manganese in the leachate and the concentrations of chromium, iron, and sodium in the solubilized extract, complying with the toxicity and drinking water standards recommended by the USEPA. However, it also increased the concentration of aluminum in both extracts, exceeding the limit set by CONAMA 460 (Brazilian standard).

1. Introduction

The management and storage of mining tailings have received special attention worldwide due to the human, economic, and environmental risks associated with some storage structures, amplified by incidents like the upstream tailings dam failures at the end of the last decade, such as Brumadinho and Mariana (Bruschi et al., 2021; Williams, 2021; Consoli et al., 2022a; Cacciuttolo & Atencio, 2023; Tian et al., 2023).

Beyond catastrophic failures, authors such as Liu et al. (2005), Mileusnić et al. (2014), and Khoeurn et al. (2019) identified leaching from mine tailings releases hazardous metals that may cause soil and water contamination by toxic metals. Recently, Saraiva et al. (2024) showed in their study that children living in communities exposed to mining dust in Brumadinho, Brazil, are three times more likely to have respiratory allergies than children in areas not exposed. Hansen (2015) reported that the effluents from tailings Dams in Witwatersrand are acidic and contain elevated concentrations of trace metals and sulfate (SO_4). Regarding bauxite tailings, Ghosh et al. (2011) showed the potential for contaminant leaching, and Päivärinta-Antikainen et al. (2023) found that the elements leaching from bauxite tailings may induce toxicity in human cells.

Advances in dewatering technologies have resulted in the development of disposal methods based on mine tailings filtration and compaction, such as dry stacking tailings as an alternative to hydraulically depositing in dams. (Consoli, et al., 2022b; Rissoli et al., 2024). Additionally, there is consideration of adding a binder to the mine tailings before stacking to improve the mechanical and environmental properties of the material (Choi et al., 2009; Bruschi et al., 2022; Levandoski et al., 2024; Santos et al.,

#Corresponding author. E-mail address: carina.silvani@professor.ufcg.edu.br
[1]Universidade Federal de Campina Grande, Unidade Acadêmica de Engenharia Civil, Campina Grande, PB, Brasil.
[2]ALUMAR - Consórcio de Alumínio do Maranhão S.A., São Luís, MA, Brasil.
[3]Centro Universitário Maurício de Nassau, São Luís, MA, Brasil.
[4]Universidade Federal de Mato Grosso, Departamento de Engenharia Civil, Cuiabá, MT, Brasil.

Submitted on June 26, 2025; Final Acceptance on March 20, 2026; Discussion open until February 27, 2027.
Editor: Renato P. Cunha
https://doi.org/10.28927/SR.2026.010225

2025). In this context, the use of small amounts of binding agents like Portland cement has the potential to facilitate the bauxite tailings disposal sites, which leads to increased strength, allowing the embankment to be steeper, reducing the land needed for storage of the tailings (Consoli, et al., 2022b; Farenzena et al., 2024). Therefore, understanding the mechanical response of stabilized ore tailings and the establishment of dosage methodologies for mining tailings is crucial for their use as a geomaterial and for ensuring safe stacking.

Based on laboratory tests, Consoli et al. (2022b) found that unconfined compression strength (q_u) can be related to the porosity/volumetric cement content (η/C_{iv}) for iron ore tailings. This index has been successfully related to unconfined compression strength (q_u) and splitting tensile strength (q_t) for several sandy soils and tailings (Consoli et al., 2009, 2010, 2014). Studies such as Bruschi (2020) and Bruschi et al. (2021) have shown that the results of q_u and q_t of fine-grained bauxite tailings stabilized with Portland Cement can successfully be adjusted based on the η/C_{iv} index for Portland cement contents higher than 15%.

While q_u and q_t are important, shear strength parameters are essential for the safe and efficient design of cemented dry stacking tailings. Nevertheless, triaxial test results are often difficult to obtain or not readily available. To address this challenge, researchers such as Mitchell (1981), Schnaid et al. (2001) and Consoli (2014) have employed unconfined strength tests to estimate shear strength parameters for cemented and uncemented soils. Consoli et al. (2014) demonstrated that the effective angle of shearing resistance (ϕ') of a given cemented sandy soil can be determined using the q_t/q_u relationship, while the effective cohesion intercept (c') is directly related to q_u. Carvalho et al. (2023) successfully used this approach to predict iron ore tailing strength parameters. Despite the research presented, this research presents novelty in the application of η/C_{iv} approach for BT collected close to the launching point, characterized by a sandier granulometry and stabilized with low Portland cement contents ($C_i \leq 6\%$) to forecast q_u, q_t, ϕ' and c' together with an environmental analysis. It combines a practical, efficient method for evaluating the strength of cement-bauxite tailings mixtures (using realistic cement contents) with an environmental perspective that considers current legislation and the demands of the mining sector.

Therefore, this study aims to evaluate the geomechanical and environmental performance of bauxite tailings (BT) stabilized with Portland cement for application in cemented dry tailings piles.

2. Materials and methods

2.1 Materials

The BT was collected from a deposit area in Maranhão, northeast of Brazil, at a depth of 1 m next to the launch point. The BT originates from bauxite ore processing, which follows the Bayer process and was released into the deposit in liquid form. Gravitational separation occurred, with the coarsest grains remaining close to the launch point (James, 2018; Sandroni & Guidicini, 2022). This deposit area was operational from 2017 to 2019. In the laboratory, the BT was dried at 105 °C without undergoing a sieving process and then stored in plastic bags. According to the Unified Soil Classification System (USCS) (ASTM, 2017), the BT is classified as non-plastic silty sand (SM). The grain size distribution, presented in Figure 1, indicates a predominance of coarse grains (approximately 70%). The binder used was high early strength (Type III) Portland cement with a specific gravity (G_s) of 2.99 g/cm^3. Additionally, distilled water was used in the molding process.

Mineralogical analysis was conducted using a Bruker D2 Phaser diffractometer, with testing performed in the angular range of 3° to 70° 2θ at a step size of 0.02° and copper cathode. The X-ray diffraction (XRD) results (Figure 2) show that BT is predominantly composed of sodalite ($Na_8(Al_6Si_6O_{24})Cl_2$), hematite (Fe_2O_3), gibbsite ($Al(OH)_3$), and quartz (SiO_2). The chemical composition was determined by X-ray fluorescence (XRF) analysis using a Shimadzu ERX-720 Spectrometer with a copper cathode and revealed that the BT contains substantial amounts of Na_2O, Fe_2O_3, Al_2O_3, and SiO_2 (Table 1). The G_s of BT is 3.32 g/cm^3, according to ASTM D5550 (ASTM, 2014), and this high value can be attributed to the high content of Fe_2O_3. The pH of the bauxite tailings in H_2O was 10.46, according to ASTM D4972 (ASTM, 2024b). Additionally, results of the specific surface area using the blue methylene index, according to ASTM C837 (ASTM, 2019), indicate a low specific surface area of 48.79 m^2/g, which is expected due to the absence of clay minerals.

The BT was classified according to the Brazilian normative for waste classification the NBR 10004 (ABNT, 2004a). In this process was the BT went thought solubilization test (ABNT, 2004c, d), which according to the Annex G of NBR 10004 it can be classified as non-inert material, for exceed some metals such as Al, Cr and Fe. After that leachability test

Table 1. Chemical composition of the BT.

Chemical properties	
Sample	Bauxite tailings
pH	10.46
Specific surface area (m^2/g)	48.79
Na_2O (%)	30.21
Fe_2O_3 (%)	25.29
Al_2O_3 (%)	24.24
SiO_2 (%)	11.49
TiO_2 (%)	1.94
ZrO_2 (%)	0.43
Others (%)	0.56
*LOI** (%)	5.83

**LOI*, loss on ignition (1000 °C).

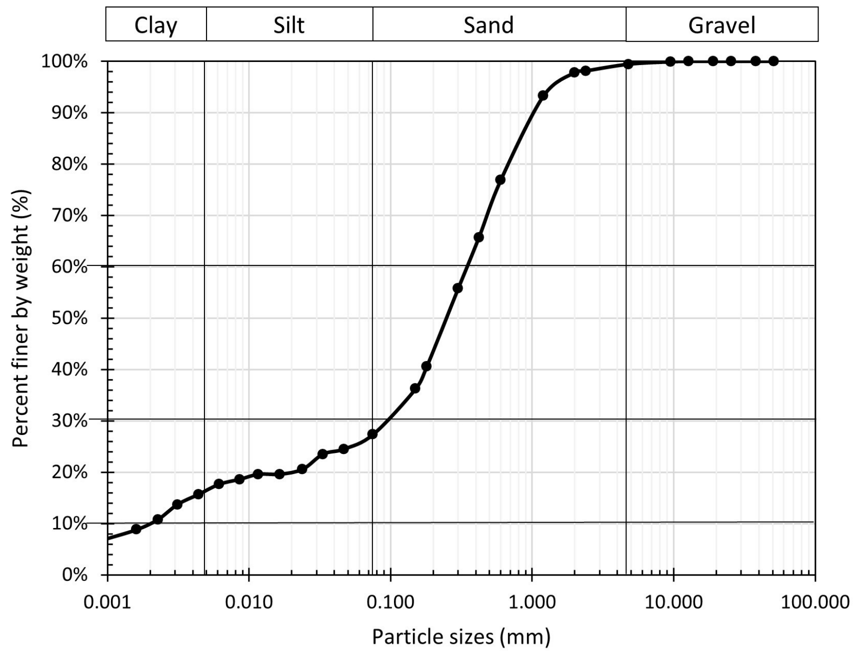

Figure 1. Grain size distribution of the BT.

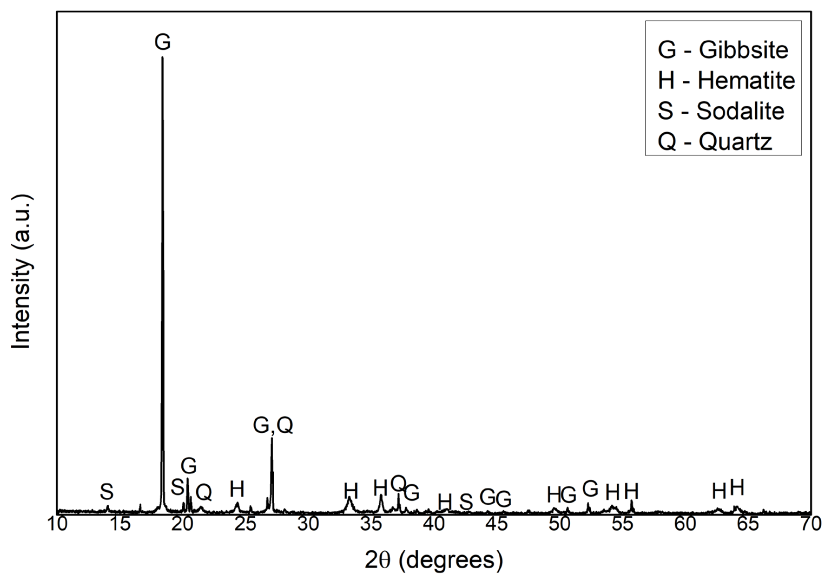

Figure 2. XRD of bauxite tailings.

results (ABNT, 2004b) showed that the BT does not exceed any limit of the Annex F of NBR 10004 (ABNT, 2004a). Therefore, the BT was classified as a Non-Hazardous waste.

2.2 Experimental program

The experimental program was divided into five parts. The first part involved the characterization of the BT and Portland cement. The second part focused on the mechanical analysis of BT-cement mixtures through unconfined compressive strength (UCS), splitting tensile strength (STS) tests, and consolidated undrained triaxial (CIU) tests. The third part involved leachability and solubilization testing. The fourth part consisted of a statistical analysis of the q_u and q_t results at a significance level (α) of 5%. Finally, the last part assessed the feasibility of predicting the cohesion (c) and angle of internal friction (ϕ) of the blends using q_u and q_t.

Portland cement content was set at 2%, 4%, and 6% based on values typically used in the literature. Research such as Consoli et al. (2022b), Chaves et al. (2025) and Scheuermann Filho & Consoli (2024) among others, have shown that values of the order of 6% or less are satisfactory to stabilize mining tailings. The γ_d were defined as 18 kN/m^3, 19 kN/m^3, and 20 kN/m^3, and the water content of the test specimens was set at 18%, based on the compaction test (Figure 3) on standard energy for BT (ASTM 2021).

Table 2 presents all the experimental programs. The UCS and STS tests were done for all C_i and γ_d to investigate the influence of the cement content and porosity on the strength of BT-Cement. CIU triaxial tests were conducted on both untreated BT and BT mixed with 2% Portland cement, compacted at 20 kN/m^3 with a water content of 18%. The Portland cement content was set at 2% to reduce costs and minimize greenhouse gas emissions associated with the technique. The leachability and solubilization tests were conducted on specimens with 20 kN/m^3 and C_i of 0%, 2%, and 6% to evaluate the impact of Portland cement on metal encapsulation. The curing time was 7 days for all samples because, from a practical point of view, the most cementing reactions of the PC type III have occurred at this period, and a pile can be delivered for traffic.

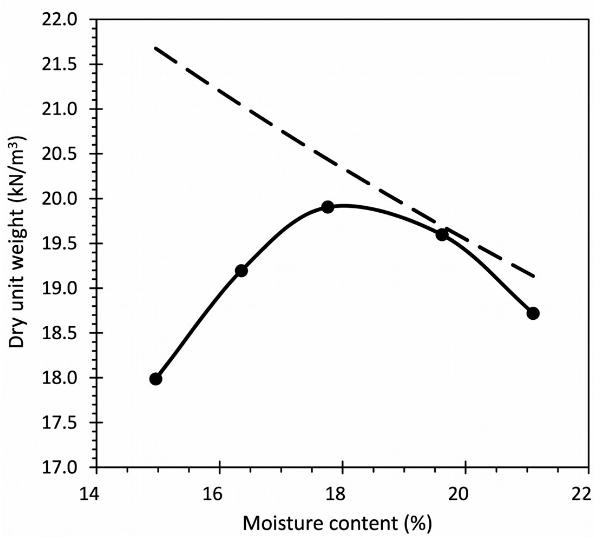

Figure 3. Compaction test of bauxite tailings.

2.3 Methods

2.3.1 Molding and curing specimens

Cylindrical specimens with a diameter of 50 mm and a height of 100 mm were utilized for UCS, STS, and Triaxial tests. The specimens were prepared manually by mixing dry BT, cement, and water. The specimens were statically compacted in three layers, and between them, the top was slightly scarified. With the specimens done, they were weighed with 0.01 g accuracy and measured with a precision of 0.01 mm. The samples were accepted if they followed these limits: dry unit weight ±1%, moisture content ±0.5%, and dimensions within ±1% of the specified values. The samples for UCS and STS tests were cured for six days in a humid room at 23 °C ± 2 °C, and on the sixth day, they were soaked in water for 24 hours to minimize suction effects (Consoli et al., 2011), bringing the time curing to 7 days. For the leachability and solubilization test, cylindrical specimens were molded in the same condition as the samples for mechanical tests (Table 2), cured for 7 days.

Table 2. Experimental design.

Test	γ_d (kN/m^3)	Cement content (%)	Number of samples
Unconfined compressive strength/split tensile strength	18	2	3
		4	3
		6	3
	19	2	3
		4	3
		6	3
	20	2	3
		4	3
		6	3
Leaching	20	0	1
		2	1
		6	1
Solubilization	20	0	1
		2	1
		6	1
CIU Triaxial tests	20	0	3
		2	3

2.3.2 UCS and STS tests

UCS tests were executed in accordance with ASTM D2166 (ASTM, 2024a), and the STS tests were performed in accordance with NBR 7222 (ABNT, 2004c). Both tests were performed in an automatic loading machine, with a maximum load capacity of 100 kN; the rate of displacement adopted was 1.14 mm per minute. Additionally, for UCS and STS results, statistical analyses were conducted using analysis of variance (ANOVA) and Tukey's multiple comparison test (MCT).

2.3.3 Porosity/Portland cement content index

The unconfined compressive strength (q_u) and splitting tensile strength (q_t) are expressed as functions of the porosity/volumetric content of cement index proposed by Consoli et al. (2017a) and adapted for the material used in this research in Equations 1 and 2.

Porosity (η) is obtained as the ratio of the volume of voids to the total volume of the specimen. It is a function of dry unit weight (γ_d) of the mixture, Portland cement content (C_i), bauxite tailings content (BT), total volume of the specimen (Vs), and the unit weight of solids of BT(γ_{sBT}) and Portland cement(γ_{sCi}). The volumetric Portland cement content (C_{iv}) is the result of the volume of Portland cement (cement mass (m_{Ci}) divided by γ_{sCi} divided by V_s. Through the index $\eta/C_{iv,}$ it becomes possible to unify the data into a single equation, providing a dosing method for the stabilized mixtures studied here.

$$\eta = 100 - 100\left\{\left[\frac{\gamma_d}{1+\frac{C_i}{100}}\right]\times\left[\frac{1}{\gamma_{sBT}}+\frac{C_i}{\gamma_{sCi}}\right]\right\} \tag{1}$$

$$C_{iv} = \frac{V_{Ci}}{V_s} = \frac{m_{Ci}/\gamma sC_i}{V_s} \tag{2}$$

2.3.4 Triaxial test

Isotropically consolidated undrained (CIU) triaxial tests were conducted in accordance with the ASTM D4767 standard (ASTM, 2020). To ensure complete saturation of each test specimen, a three-step process was employed: (i) CO_2 percolation, (ii) distilled water percolation, and (iii) the application of incremental backpressure until achieving a *B-value* greater than 0.95. The undrained shearing was performed in a strain-controlled manner at a rate of 0.06 mm per hour. Tests were conducted at confining pressures of 100, 200, and 300 kPa.

2.3.5 Leaching and solubilization tests

The leaching and solubilization tests, according to Brazilian standards for solid waste characterization (ABNT, 2004a, b, c, d), were used to assess the lixiviation of BT, and BT with the addition of Portland cement. The solubilization test was used as a complementary test, based on the premise - supported by the literature - that it simulates events related to water infiltration or groundwater interaction beneath a stabilized dry-stacked tailings deposit (Wang et al., 2022; Morais et al., 2023). Solid waste characterization methods are commonly used to assess metal leaching from Portland cement-stabilized material (Mahedi & Cetin, 2019; Chinyama et al., 2023; Wang et al., 2023).

For the leaching test, first the specimens crushed to smaller particles (9.5 mm), than were exposed to acetic acid solution (*pH*~2.88) with a solid/liquid ratio of 1:20. The mixture was agitated in a rotary shaker at 30 rpm and 23 ± 2°C for 18±2 h, according to NBR 10005 (ABNT, 2004b) and described by Ferrazzo et al. (2023). For solubilization tests, 250 g of the crushed samples (9.5 mm) was added to the 1500 ml bottle with 1000 ml of distilled water and rotated at low speed for 5 min. Then the mixture was left to rest for 7 days at 25 °C. The leached and solubilized extracts were filtered through a 0.45μm membrane filter to remove the suspended solids, according to procedure 3030E (APHA, 2017).

The analysis for Silver (Ag), Aluminum (Al), Arsenic (As), Barium (Ba), Cadmium (Cd), Chromium (Cr), Copper (Cu), Iron (Fe), Mercury (Hg), Manganese (Mn), Lead (Pb), Selenium (Se), and Zinc (Zn) was performed according to the procedure 3120B (APHA, 2017), using inductively coupled plasma atomic emission spectrometry (Shimadzu-branded ICP-AES) with standard curves prepared from a mono-element solution (elements in dilute nitric acid, HNO_3). The results were then compared with environmental standards and regulations such as ABNT NBR 10004 (ABNT, 2004a), CONAMA 460 (Brasil, 2013) and USEPA (2025).

3. Results and discussion

3.1 Effect of porosity/cement volumetric content index (η/C_{iv}) on q_u and q_t

The q_u and q_t results were correlated with (η/C_{iv}) using a power-type relationship (Figure 4), revealing an inverse trend between the evaluated mechanical properties and the η/C_{iv} parameter. Therefore, higher strength was observed in specimens with greater compaction and higher cement content. Sufficient correlations (R^2>0.92) were achieved using power functions (Equations 3 and 4). These equations have the general form of Equation 5. To align the effects of porosity (η) and the inverse of the cement volumetric content ($1/C_{iv}$) with q_u and q_t an adjusted internal exponent (k) was set at 1. A value of k equal to 1 has been used in previous studies (Consoli et al., 2022a; Servi et al., 2022) to correlate the mechanical performance, through the η/C_{iv} index, of geomaterials exhibiting frictional behavior when artificially cemented. Like BT, these materials are primarily

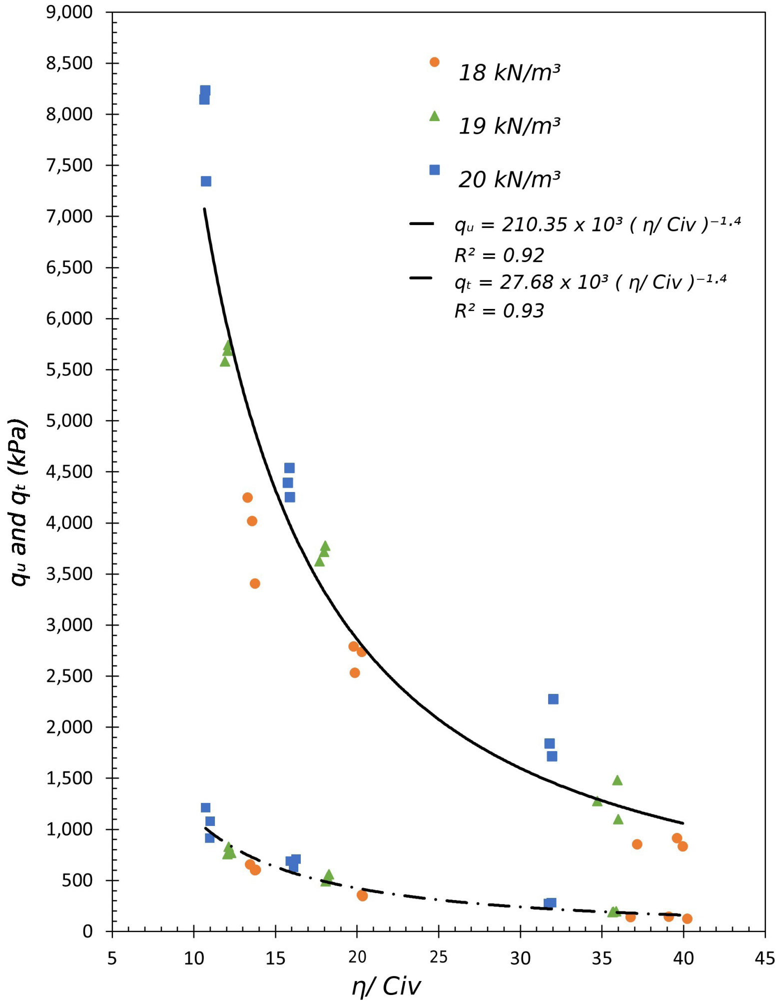

Figure 4. Mechanical strength results as a function of the η/C_{iv} index.

composed of sand particle fractions (from fine to coarse) and/or have a high content of non-plastic fines. Additionally, the comparatively high value of the power k indicates a significant contribution of Portland cement content to q_u and q_t.

$$q_u = 210.35 \times 10^3 \times \left(\frac{\eta}{C_{iv}}\right)^{-1.4} ; R^2 = 0.92 \quad (3)$$

$$q_t = 28.20 \times 10^3 \times \left(\frac{\eta}{C_{iv}}\right)^{-1.4} ; R^2 = 0.93 \quad (4)$$

$$q_u \; or \; q_t \left(kPa\right) = D^* \left(\frac{\eta}{C_{iv}{}^k}\right)^E \quad (5)$$

Similarly, using an external exponent (E) with a constant value of 1.4, determined through curve fitting, it can be verified that only the magnitude of the scalar "D" changes in each of the proposed power functions (Equations 3 and 4). It is important to point out that Diambra et al. (2018) stated that k is inversely related to the E (1≅1/1.4). Therefore, q_u and q_t of stabilized BTs can be compared for the different compaction densities and Portland cement contents.

Consoli et al. (2010, 2012) have shown that for each type of cemented soil, there is a unique relationship between the q_t and q_u. This relationship is represented by a single scalar (ξ), independent of porosity, cement content, and the porosity/volumetric cement content index; however, it depends on the characteristics of the soil and the binder used. In the case of BT improved with Portland cement, the relationship between q_t and q_u can be obtained by dividing Equation 4 by Equation 3 (Equation 6), resulting in 0.14. These results are consistent with the range of 0.13-0.19 reported by Consoli et al. (2010, 2014) and Stracke et al. (2012), allowing the prediction of qt from the measurement of q_u.

$$\xi = \frac{q_t}{q_u} = \frac{28.20\times10^3\times\left[\dfrac{\eta}{(C_{iv})}\right]^{-1.4}}{194.55\times10^3\times\left[\dfrac{\eta}{(C_{iv})}\right]^{-1.4}} = 0.14 \qquad (6)$$

3.2 Statistical analysis

Analysis of variance (ANOVA) was applied to statistically investigate the impact of the controllable factors (i.e., γ_d and C_i) on the strength of the compacted BT improved with Portland cement. Tables 3 and 4 show the ANOVA results for q_u and q_t, respectively, with a *p-value* lower than 5%.

The variation in C_i had a more pronounced influence than changes in γ_d. For q_u results (Table 3), the impact of the γ_d was close to the effect of the C_i; higher densities tend to improve the strength at almost the same level of increase in cementation. This trend is further supported by the high sum of squares observed for the interaction between the two variables. For the q_t results (Table 4), the C_i have a greater effect, as indicated by the higher sum of squares values attributed to C_i compared to γ_d and the γ_d*C_i interaction. This behavior can be attributed to the direct relationship between the cementation process and tensile strength.

After performing the ANOVA test to identify differences between the means of the treatments, the Tukey's multiple comparison test (MCT) was applied with a 95% confidence interval. Table 5 presents the average results for each treatment for q_u and q_t, representing the mean outcomes of the test conducted in triplicate, along with the results of the Tukey test.

The means of two treatments are considered equal when they share the same reference letter. Therefore, there is no statistically significant difference between those treatments, as shown in Table 5. For example, considering q_u results, treatments 4*19, 4*20, and 6*18 are statistically the same (Reference letter A). That is, there is no statistical difference between employing 4% C_i and compacting to either 19 or 20 kN/m³, or using 6% C_i and a γ_d equal to 18 kN/m³ when evaluating q_u. Similarly, the same pattern was found for q_t results, where the treatments 4*19, 4*20, and 6*18 are statistically equal (Reference letter C). In other words, similar q_t/q_u responses can be achieved using different dosages, confirming the distinct power-type relationship that describes the q_t/q_u response of all samples as a function of the η/C_{iv} index (Figure 4).

Table 3. ANOVA table for the unconfined compression strength results.

Source	Sum of squares	Degrees of freedom	Mean Squares	*p*- value	Significant
γ_d (kN/m³)	2.31x107	2	1.16x107	< 0.001	Yes
C_i (%)	8.94x107	2	4.47x107	< 0.001	Yes
γ_d (kN/m³) * C_i (%)	7.36x106	4	1.84x106	< 0.001	Yes
Residues	1.22x106	18	67,510	-	-

Table 4. ANOVA table for the split tensile strength results.

Source	Sum of squares	Degrees of freedom	Mean Squares	*p*- value	Significant
γ_d (kN/m³)	423,816	2	211,908	< 0.001	Yes
C_i (%)	1.74x106	2	868,614	< 0.001	Yes
γ_d (kN/m³) * C_i (%)	76,704	4	19,176	0.003	Yes
Residues	55,520	18	3,084	-	-

Table 5. Data from Tukey's multiple comparison test for q_u *and* q_t.

C_i*γ_d	UCS		STS	
	Mean q_u (kPa)	Reference letter	Mean q_t (kPa)	Reference letter
2*18	868.38	B	138.27	A
2*19	1285.83	B, C	193.97	A, B
2*20	1943.89	C	280.90	A, B
4*18	2687.98	D	351.62	B
4*19	3706.26	A	527.37	C
4*20	4394.38	A	677.84	C, D
6*18	3890.36	A	621.37	C
6*19	5671.14	E	785.43	D
6*20	7907.48	F	1070.28	E

3.3 Triaxial results

CIU triaxial tests were conducted to evaluate the stress-strain behavior of BT and BT stabilized with 2% cement with γ_d of 20 kN/m^3 and water content of 18%. For the BT, the stress-strain curves (Figure 5) showed no well-defined peak at rupture. The specimens did not exhibit a sudden strength drop post-failure or a distinct failure plane, indicating the material retained some load-bearing capacity after failure, characteristic of ductile behavior. The material initially generates positive pore-pressure at all studied confining pressures, followed by a significant negative pore-pressure response, indicating that it is not susceptible to liquefaction. Figure 6a contains the peak-strength envelope that resulted in a peak angle of shearing strength (ϕ'_{peak}) around 43.1° and cohesion intercept (c'_{peak}) of 0 kPa. This behavior agrees with the literature, although undisturbed ore tailings samples coming from dams present contractive behavior (or generation of positive pore-pressure) as presented by Newson et al. (2006) and Gonçalves et al. (2024), tailings dewatered and mechanically compacted, as those used in dry stacking tailings, present dilative behavior (creation of negative pore-pressure) as reported by Carvalho et al. (2023), Wagner et al. (2023), and Bruschi et al. (2023). Therefore, BT dewatered and compacted presents better behavior than mud BT tailings, especially when considering liquefaction.

Figure 5 shows that cemented BT samples exhibited a distinct peak followed by a sharp stress drop after rupture, indicating brittle behavior. This response was marked by the formation of well-defined shear planes, characteristic of cemented granular materials. Initially, the specimens displayed stiff behavior with contraction, which was later followed by a strain-softening response and a dilative trend. The peak failure envelopes and the ultimate failure envelopes are depicted in Figure 6b. The ϕ'_{peak} for cemented BT is around 47.9° and c'_{peak} is 94.2 kPa. The critical state friction angle (ϕ'_{cs}) is 43.8°. For both cemented and uncemented BT, increased confining pressure enhanced peak strength and material stiffness, aligned with observations by Gonçalves et al. (2024), Bruschi et al. (2023), and Carvalho et al. (2023) for confining pressure lower than 500 kPa.

The addition of 2% Portland cement fundamentally transformed the behavior of BT from a purely frictional response to a cohesive-frictional one, with a significant portion of strength deriving from the cement matrix. These improvements align with the design requirements for filtered tailings in dry stacking, facilitating the construction of taller and steeper tailings stacks. Similar results were found by

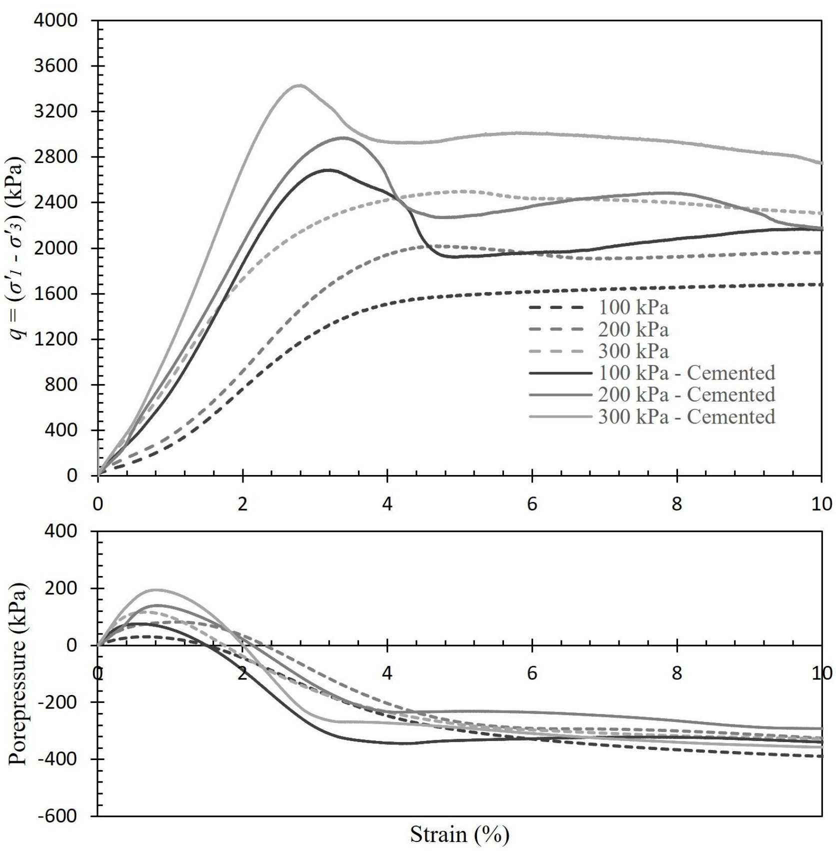

Figure 5. Stress-strain behavior of uncemented and cemented (2% of Portland cement) bauxite tailings.

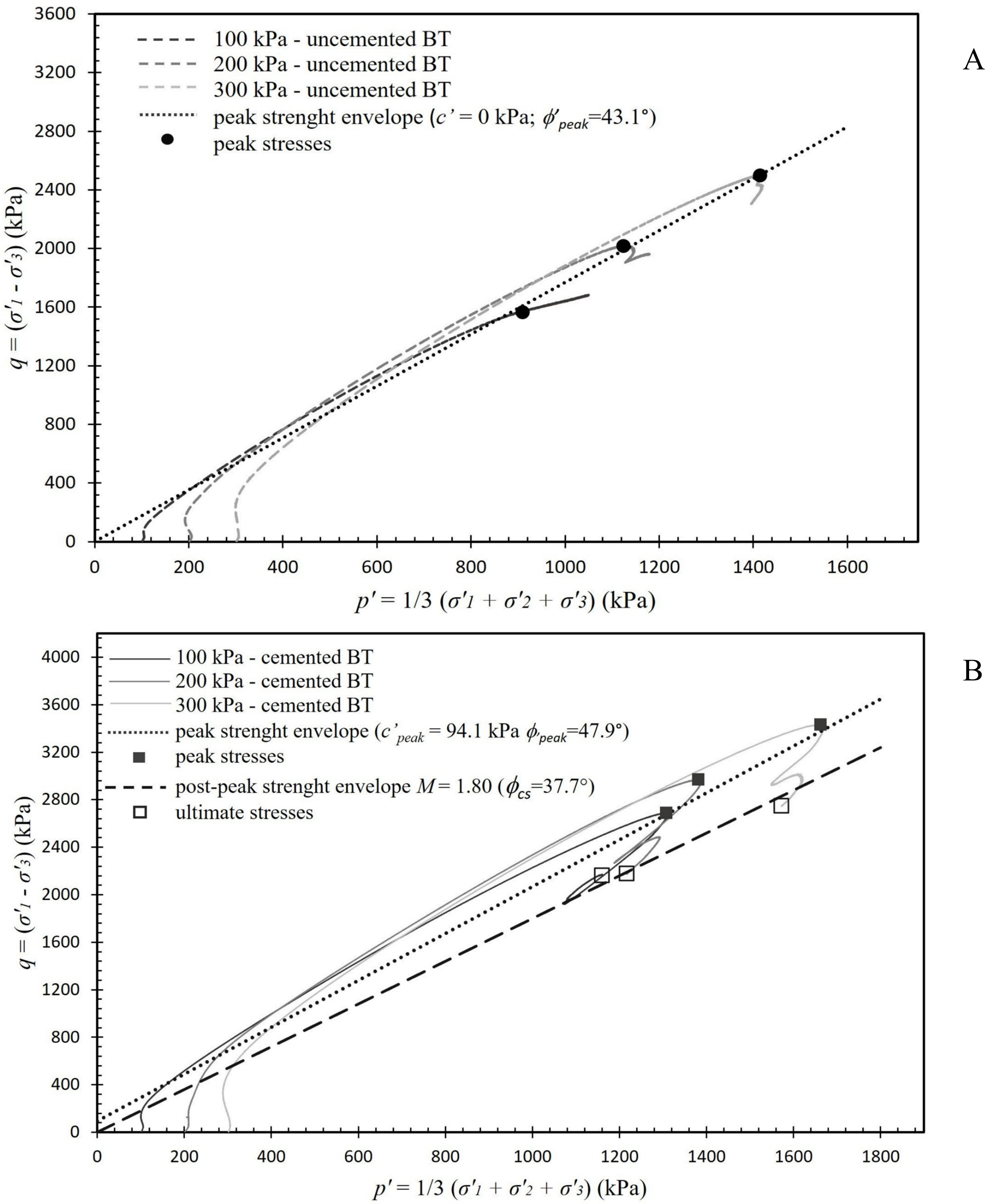

Figure 6. Stress paths and strength envelopes for: (A) bauxite tailings; (B) Cemented bauxite tailing containing 2% of PC III.

Carvalho et al (2023) for dewatered and compacted iron ore tailings.

3.4 Design parameters of cemented BT estimation by q_u and q_t

To establish a relationship between simple tests (UCS and STS) and the triaxial test outcomes of cemented BT, the approach presented by Consoli (2014) was evaluated. This approach assumes that adding a certain amount of cement to the soil does not significantly alter the peak friction angle (ϕ'_{peak}) but induces considerable changes in the effective cohesion (c'_{peak}). Therefore, Equations 7 and 8 can be used to estimate ϕ'_{peak} and c'_{peak} respectively.

$$\phi'_{peak,est} = arcsin\left(\frac{1-4\xi}{1-2\xi}\right) \quad (7)$$

$$c'_{peak,est}\left(kPa\right)=\frac{q_u\left[1-\left(\frac{1-4\xi}{1-2\xi}\right)\right]}{2\,cos\left[sin^{-1}\left(\frac{1-4\xi}{1-2\xi}\right)\right]} \tag{8}$$

where ξ is the ratio between the q_t and q_u of the cemented material.

As presented in Equation 6, the q_t/q_u ratio for cemented BT is 0.14, so the estimated peak friction angle ($\phi'_{peak,est}$) calculated by Equation 7 is 37.7°.

Equation 8 can be extended by replacing q_u with Equation 3, resulting in Equation 9. The estimated cohesion intercept ($c'_{peak,est}$) was calculated for blends with 2% Portland cement and a dry unit weight of 20 kN/m^3 (η/C_{iv} = 31.92) to ensure comparability with the triaxial test results, yielding a $c'_{peak,est}$ of 396.68 kPa. Figure 7 compares the estimated failure envelope with the failure envelope obtained from triaxial tests.

$$c'_{peak,est}\left(kPa\right)=\frac{210.35\times10^{3}\times\left(\frac{\eta}{C_{iv}}\right)^{-1.4}\left[1-\left(\frac{1-4\xi}{1-2\xi}\right)\right]}{2\,cos\left[sin^{-1}\left(\frac{1-4\xi}{1-2\xi}\right)\right]} \tag{9}$$

Accordingly, the peak-strength envelopes of the artificially cemented BT, at specific dosages, can be estimated if both the q_t/q_u ratio and η/C_{iv} are available. In this case, this approach showed an overestimation of c'_{peak} and an underestimation of $\phi'_{peak,est}$ compared to the experimental results, similar behavior was observed by Consoli et al. (2017b). Although the methodology has certain limitations, it is a useful preliminary estimation, particularly for viability analysis and the pre-project phase of dry-stacking tailings.

3.5 Leachability and solubilization analysis

The analysis for the leachate extracts is presented in Table 6, values in bold correspond to concentrations that exceeded the limits of one or more standards. The addition of Portland cement increases the leachability of Al, Fe, and Zn, although the concentration of Fe and Zn remains within regulatory limits. This increase in Al, Fe, and Zn can be attributed to the composition of the Portland Cement, where the presence of these elements is expected. According to Tang et al. (2023) and Wang et al. (2022), in cementation process, production of C–S–H gel, and release of $Ca(OH)_2$, ettringite crystal ($Ca_6Mn_2(SO_4)_2(SO_3)_2(OH)_{12}\cdot 24H_2O$) can be formed in the system substituting Al ions with Mn ions for stable solidification, what could in increase the concentration of Al in leachability extracts and contribute to the Mn encapsulation. Additionally, according to Tang et al. (2023), the high surface area of C–S–H gel promotes physisorption, as positively charged ions such as Mn^{2+} are attracted to the negatively charged surfaces of C–S–H. Consequently, C–(A)–S–H structures are capable of physically adsorbing Mn^{2+}

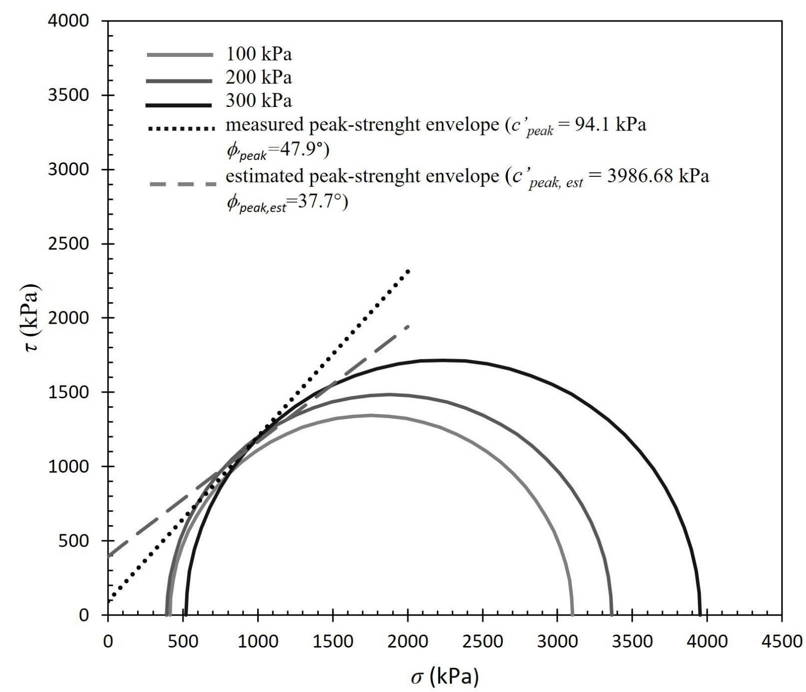

Figure 7. Comparison between Mohr-Coulomb failure envelope according to triaxial testing and Consoli (2014).

within the hardened matrix. Still, further studies should be conducted to better understand the leachability of compounds derived from cementation itself.

Table 6 shows that the cement-stabilized BT does not exhibit metal toxicity based on the leaching test results, as the concentrations of metals do not exceed the limits established in Annex F of ABNT NBR 10004 (ABNT, 2004a). Additionally, the metal concentrations in the BT leachate were compared with the National Primary Drinking Water Regulations (NPDWR), which define maximum contaminant levels (MCLs) for potable water to protect public health (USEPA, 2025). The BT leachate concentrations are below these MCLs, indicating that, under these potable water standards, metal levels are comparatively low. This indicates that neither BT nor cement-stabilized BT, under field conditions, is expected to impair the potability of water bodies. Despite this, the Al concentrations exceed the limits of CONAMA 460 (Brasil, 2013) in all samples tested. According to the Brazilian guideline, such exceedance indicates potential non-compliance with groundwater quality reference values and the need for further assessment considering exposure pathways and site-specific conditions.

Table 7 shows the chemical composition of the solubilized extracts; the values in bold indicate concentrations that

Table 6. Composition of the leached extract (in mg/L^{-1}).

Element	Bauxite tailings	BT + PC content (%)		Standards		
		2	6	Annex F of NBR 10004 (ABNT, 2004a)[1]	CONAMA 460 (Brasil, 2013)[2]	USEPA (2025)[3]
Al	**7.602**	**113.9**	**121.7**	---	**3.5**	---
Ag	<0.01*	<0.01*	<0.01*	5	0.05	---
As	<0.01*	<0.01*	<0.01*	1	0.01	0.01
Ba	<0.03*	<0.03*	<0.03*	70	0.7	2
Cd	<0.001*	<0.001*	<0.001*	0.5	0.005	0.005
Cr	<0.03*	<0.03*	<0.03*	5	0.05	0.1
Cu	< 0.008	< 0.008	< 0.008	---	2	1.3
Fe	0.5759	1.351	1.837	---	2.45	---
Hg	<0.001*	<0.001*	<0.001*	0.1	0.001	0.002
Mn	0.09487	0.04627	0.043	---	0.4	---
Pb	<0.01*	<0.01*	<0.01*	1	0.01	0.015
Se	<0.01*	<0.01*	<0.01*	1	0.01	0.05
Zn	0.07419	0.2339	0.2777	---	1.05	---

*Lower than the detection limit. [1]Brazilian standard for solid waste classification. [2]Guiding values of groundwater and drinking water. [3]Maximum contaminant levels—national primary drinking water regulations.

Table 7. Composition of the solubilized extract (in mg/L^{-1}).

Element	Bauxite tailings	BT + PC content (%)		Standards		
		2	6	Annex G of NBR 10004 (ABNT, 2004a)[1]	CONAMA 460 (Brasil, 2013)[2]	USEPA (2025)[3]
Al	**12.27**	**16.8**	**23.15**	**0.2**	**3.5**	-
Ag	< 0.01*	< 0.01*	< 0.01*	0.05	0.05	-
As	< 0.01*	< 0.01*	< 0.01*	0.01	0.01	0.01
Ba	< 0.03*	< 0.03*	< 0.03*	0.7	0.7	2
Cd	< 0.001*	< 0.001*	< 0.001*	0.005	0.005	0.005
Cr	**0.2549**	0.03	<0.03*	**0.05**	**0.05**	**0.1**
Cu	< 0.008*	< 0.008*	< 0.008*	2	2	1.3
Fe	**1.775**	0.2019	0.08243	**0.3**	2.45	-
Hg	< 0.001*	< 0.001*	< 0.001*	0.001	0.001	0.002
Mn	< 0.02*	< 0.02*	< 0.02*	0.1	0.4	-
Na	191.4	136.5	52.4	200	---	-
Pb	< 0.01*	< 0.01*	< 0.01*	0.01	0.01	0.015
Se	< 0.01*	< 0.01*	< 0.01*	0.01	0.01	0.05
Zn	< 0.04*	< 0.04*	< 0.04*	5	1.05	-

*Lower than the detection limit. [1]Brazilian standard for solid waste classification. [2]Guiding values of groundwater and drinking water. [3]Maximum contaminant levels—national primary drinking water regulations surpassed the limits of one or more standards. Adding small amounts of cement, elements such as Cr, Fe, and Na were effectively encapsulated. Regarding the encapsulation of Cr, it led to a reduction of solubility, so BT-Portland cement blends achieve the water potability levels preconized by USEPA (2025). Despite the addition of Portland cement, it was ineffective in encapsulating Al, as the concentration of Al increased in the solubilization extract, with the growth of C_i. It's important to note that traditional cement is mainly made up of aluminates, which contribute to the higher concentration of Al in the mixtures (Bruschi et al., 2022).

4. Conclusions

The present study investigated the mechanical and environmental performance of compacted bauxite tailings–Portland cement mixtures, from which the following conclusions were drawn:

- The porosity/volumetric content of cement (η/C_{iv}) index proves to be an appropriate parameter for evaluating the mechanical properties of cemented BT, indicating that higher η/C_{iv} ratios correspond to lower strengths. The ANOVA analysis and Tukey's test confirmed the factors that influence the strength and validated the hypotheses. The η/C_{iv} index, combined with the ratio of unconfined compressive strength to splitting tensile strength, enables the estimation of $c'_{p_{ea}k}$ and $\phi'_{p_{ea}k}$ for cemented bauxite tailings. This estimation can assist in viability studies and the pre-project phase of dry stack tailings;
- Dewatered and compacted bauxite tailings generate negative pore-pressure during shearing, reducing the risk of liquefaction. The addition of 2% Portland cement transforms the behavior of bauxite tailings from purely frictional ($c'_{p_{ea}k} = 0$) to cohesive-frictional, with $c'_{p_{ea}k}$ reaching 94.1 kPa. This enhancement enables the construction of taller and steeper stacks;
- The addition of Portland cement to bauxite tailings promoted reductions in the concentration of Manganese in the leached extract and the concentration of Chromium, Iron, and Sodium in the solubilized extract. However, it also increased the concentration of Aluminum in both extracts, exceeding the limits set by the Brazilian standard CONAMA 460. Still, adding small amounts of Portland cement to bauxite tailings can make it adequate to the toxicity and water potability levels preconized by USEPA.

Portland cement improves the mechanical behavior of Bauxite tailings; nonetheless, it has some limitations in fully encapsulating the toxic components of Bauxite tailings, so future studies have room for solutions to mitigate those environmental concerns, particularly through the use of alternative binders based on alkali-activation approaches.

Acknowledgements

The authors wish to express their gratitude to ALCOA ALUMÍNIO S/A and the Coordination for the Improvement of Higher Level Education Personnel (CAPES) for the financial support to the research group.

Declaration of interest

The authors have no conflicts of interest to declare. All co-authors have observed and affirmed the contents of the paper and there is no financial interest to report.

Authors' contributions

Gilson Gabriel Teixeira Varela: data curation, methodology, visualization, formal analysis, writing – original draft. David Braga Fernandes: funding acquisition, project administration, resources. Aldenora Vieira Santos Neta: funding acquisition, project administration, resources. Alisson do Nascimento Lima: data curation, methodology, formal analysis, writing – review & editing. Lara Pereira Tavares Mendes: methodology, visualization, formal analysis. Manoel Leandro Araújo e Farias: methodology, visualization, formal analysis. Carina Silvani: conceptualization, supervision, validation, writing – review & editing.

Data availability

The datasets generated analyzed in the course of the current study are available from the corresponding author upon request.

Declaration of use of generative artificial intelligence

This work was prepared without the assistance of any generative artificial intelligence (GenAI) tools or services. All aspects of the manuscript were developed solely by the authors, who take full responsibility for the content of this publication.

List of symbols and abbreviations

c	cohesion
$c'_{peak,est}$	Estimated cohesion intercept
m_{Ci}	total volume of the specimen
p'	Effective stress
q_u	unconfined compression strength
q_t	splitting tensile strength
ABNT	Associação Brasileira de Normas Técnicas
ASTM	American Society for Testing and Materials
BT	Bauxite Tailings
C–A–S–H	Calcium Aluminosilicate Hydrate

CAPES	Coordination for the Improvement of Higher Level Education Personnel
Cc	Coefficient of curvature
C_{iv}	volumetric cement content
CIU	Isotropically consolidated undrained triaxial test
CONAMA	Brazilian National Environment Council
C–S–H	Calcium Silicate Hydrate
Cu	coefficient of uniformity
G_s	Specific gravity
ICP-AES	Inductively Coupled Plasma Atomic Emission Spectroscopy
LOI	loss on ignition
MCL	maximum contaminant level
MCT	Tukey's multiple comparison test
NPDWR	National Primary Drinking Water Regulations
NBR	Brazilian Standard
PC	Portland cement
R^2	Coefficient of Determination
STS	splitting tensile strength test
SM	silty sand
USEPA	United States Environmental Protection Agency
UCS	unconfined compressive strength test
V_s	total volume of the specimen
XRD	X-ray diffraction
XRF	X-ray fluorescence
α	significance level
γ_d	dry unit weight
γ_{sBT}	unit weight of solids of Bauxite Tailings
γ_{sCi}	unit weight of solids of cement Portland
ϕ	angle of internal friction
ϕ'	effective angle of shearing resistance
ϕ'_{peak}	Peak angle of shearing strength
ϕ'_{cs}	Critical state friction angle
$\phi'_{peak,est}$	Critical state friction angle
η/C_{iv}	index porosity/volumetric cement content
η	porosity
ξ	scalar resulting from the ratio between q_t and q_u

References

ABNT NBR 10004. (2004a). *Resíduos sólidos: classificação* (p. 71). ABNT - Associação Brasileira de Normas Técnicas, Rio de Janeiro, RJ (in Portuguese).

ABNT NBR 10005. (2004b). *Lixiviação de resíduos: procedimento* (p. 16). ABNT - Associação Brasileira de Normas Técnicas, Rio de Janeiro, RJ (in Portuguese).

ABNT NBR 7222. (2004c). *Concreto e argamassa: determinação da resistência à tração por compressão diametral de corpos de prova cilíndricos* (p. 5). ABNT - Associação Brasileira de Normas Técnicas, Rio de Janeiro, RJ (in Portuguese).

ABNT NBR 10006. (2004d). *Solubilização de resíduos: procedimento* (p. 3). ABNT - Associação Brasileira de Normas Técnicas, Rio de Janeiro, RJ (in Portuguese).

American Public Health Association – APHA. (2017). *Standard methods for the examination of water and wastewate*r (23rd ed.). New York: APHA.

ASTM D5550-14. (2014). *Standard test method for specific gravity of soil solids by gas pycnometer.* ASTM International, West Conshohocken, PA. https://doi.org/10.1520/D0854-14.

ASTM D2487. (2017). *Practice for classification of soils for engineering purposes (Unified Soil Classification System).* ASTM International, West Conshohocken, PA.

ASTM C837-09. (2019). *Standard test method for methylene blue index of clay.* ASTM International, West Conshohocken, PA. https://doi.org/10.1520/C0837-09R19.

ASTM D4767-11. (2020). *Standard test method for consolidated undrained triaxial compression test for cohesive soils.* ASTM International, West Conshohocken, PA. https://doi.org/10.1520/D4767-11R20.

ASTM D698. (2021). *Standard test methods for laboratory compaction characteristics of soil using standard effort (12,400 ft-lbf/ft³ (600 kN-m/m³)).* ASTM International, West Conshohocken, PA. https://doi.org/10.1520/D0698-12R21.

ASTM D2166. (2024a). *Standard test method for unconfined compressive strength of cohesive soil.* ASTM International, West Conshohocken, PA. https://doi.org/10.1520/D2166_D2166M-16.

ASTM D4972-19. (2024b). *Standard test method for pH of soils.* ASTM International, West Conshohocken, PA. https://doi.org/10.1520/D4972-19.

Brasil. Conselho Nacional do Meio Ambiente – CONAMA. (2013). Resolução nº 460, de 30 de dezembro de 2013. Altera a Resolução nº 420, de 28 de dezembro de 2009, do Conselho Nacional do Meio Ambiente – CONAMA, que dispõe sobre critérios e valores orientadores de qualidade do solo quanto à presença de substâncias químicas e dá outras providências. *Diário Oficial [da] República Federativa do Brasil*.

Bruschi, G.J. (2020). *Stabilization of bauxite tailings through an alkali-activated system of sugarcane bagasse ash and carbide lime* [Master's dissertation]. Federal University of Rio Grande do Sul's repository (in Portuguese). Retrieved in June 26, 2025, from https://www.lume.ufrgs.br/handle/10183/218182

Bruschi, G.J., Santos, C.P., Tonini de Araújo, M., Ferrazzo, S.T., Marques, S.F.V., & Consoli, N.C. (2021). Green stabilization of bauxite tailings: mechanical study on alkali-activated materials. *Journal of Materials in Civil Engineering*, 33(11), 06021007. https://doi.org/10.1061/(ASCE)MT.1943-5533.0003949.

Bruschi, G.J., Santos, C.P., Levandoski, W.M.K., Ferrazzo, S.T., Korf, E.P., Saldanha, R.B., & Consoli, N.C. (2022). Leaching assessment of cemented bauxite tailings through wetting and drying cycles of durability test. *Environmental Science and Pollution Research International*, 29(39), 59247-59262. https://doi.org/10.1007/s11356-022-20031-5.

Bruschi, G.J., Santos, C.P.D., Scheuermann Filho, H.C., Silva Martinatto, C., Schulz, L.R., Silva, J.P.D.S., & Consoli, N.C. (2023). Mechanical and microstructural response of iron ore tailings under low and high pressures considering a wide range of molding characteristics. *Mining*, 3(4), 712-730. https://doi.org/10.3390/mining3040039.

Cacciuttolo, C., & Atencio, E. (2023). Dry stacking of filtered tailings for large-scale production rates over 100,000 metric tons per day: envisioning the sustainable future of mine tailings storage facilities. *Minerals*, 13(11), 1445. https://doi.org/10.3390/min13111445.

Carvalho, J.V.D.A., Wagner, A.C., Scheuermann Filho, H.C., Chaves, H.M., Silva, J.P.S., Delgado, B.G., & Consoli, N.C. (2023). Evaluation of strength parameters for application in cemented iron ore tailings stacks. *Indian Geotechnical Journal*, 53(4), 775-788. https://doi.org/10.1007/s40098-023-00712-9.

Chaves, L.R.C., Heineck, K.S., Scheuermann Filho, H.C., Chaves, H.M., Carvalho, J.V.A., Wagner, A.C., Silva, J.P.S., & Consoli, N.C. (2025). Field and laboratory study of iron ore tailings-Portland cement blends for dry stacking. *Geotechnical Engineering*, 178(1), 31-40. https://doi.org/10.1680/jgeen.23.00097.

Chinyama, S.R., Wenga, T., & Gwenzi, W. (2023). Mechanical and contaminant leaching behaviour of cement-based and fired bricks incorporating ferrochrome slag. *Journal of Building Engineering*, 72, 106572. https://doi.org/10.1016/j.jobe.2023.106572.

Choi, W.-H., Lee, S.-R., & Park, J.-Y. (2009). Cement based solidification/stabilization of arsenic-contaminated mine tailings. *Waste Management*, 29(5), 1766-1771. https://doi.org/10.1016/j.wasman.2008.11.008.

Consoli, N.C. (2014). A method proposed for the assessment of failure envelopes of cemented sandy soils. *Engineering Geology*, 169, 61-68. https://doi.org/10.1016/j.enggeo.2013.11.016.

Consoli, N.C., Viana da Fonseca, A., Cruz, R.C., & Heineck, K.S. (2009). Fundamental parameters for the stiffness and strength control of artificially cemented sand. *Journal of Geotechnical and Geoenvironmental Engineering*, 135(9), 1347-1353. https://doi.org/10.1061/(ASCE)GT.1943-5606.0000008.

Consoli, N.C., Cruz, R.C., Floss, M.F., & Festugato, L. (2010). Parameters controlling tensile and compressive strength of artificially cemented sand. *Journal of Geotechnical and Geoenvironmental Engineering*, 136(5), 759-763. https://doi.org/10.1061/(ASCE)GT.1943-5606.0000278.

Consoli, N.C., Rosa, A.D., & Saldanha, R.B. (2011). Variables governing strength of compacted soil–fly ash–lime mixtures. *Journal of Materials in Civil Engineering*, 23(4), 432-440. https://doi.org/10.1061/(ASCE)MT.1943-5533.0000186.

Consoli, N.C., Dalla Rosa Johann, A., Gauer, E.A., Santos, V.R., Moretto, R.L., & Corte, M.B. (2012). Key parameters for tensile and compressive strength of silt-lime mixtures. *Géotechnique Letters*, 2(3), 81-85. https://doi.org/10.1680/geolett.12.00014.

Consoli, N.C., Rocha, C.G., & Silvani, C. (2014). Devising dosages for soil–fly ash–lime blends based on tensile strength controlling equations. *Construction & Building Materials*, 55, 238-245. https://doi.org/10.1016/j.conbuildmat.2014.01.044.

Consoli, N.C., Marques, S.F.V., Floss, M.F., & Festugato, L. (2017a). Broad-spectrum empirical correlation determining tensile and compressive strength of cement-bonded clean granular soils. *Journal of Materials in Civil Engineering*, 29(6), 06017004. https://doi.org/10.1061/(ASCE)MT.1943-5533.0001858.

Consoli, N.C., Quiñónez, R.A., González, L.E., & López, R.A. (2017b). Influence of molding moisture content and porosity/cement index on stiffness, strength, and failure envelopes of artificially cemented fine-grained soils. *Journal of Materials in Civil Engineering*, 29(5), 04016277. https://doi.org/10.1061/(ASCE)MT.1943-5533.0001819.

Consoli, N.C., Silvano, L.W., Lotero, A., Scheuermann Filho, H.C., Moncaleano, C.J., & Cristelo, N. (2022a). Key parameters establishing alkali activation effects on stabilized rammed earth. *Construction & Building Materials*, 345, 128299. https://doi.org/10.1016/j.conbuildmat.2022.128299.

Consoli, N.C., Vogt, J.C., Silva, J.P.S., Chaves, H.M., Scheuermann Filho, H.C., Moreira, E.B., & Lotero, A. (2022b). Behaviour of compacted filtered iron ore tailings-Portland cement blends: new Brazilian trend for tailings disposal by stacking. *Applied Sciences*, 12(2), 836. https://doi.org/10.3390/app12020836.

Diambra, A., Festugato, L., Ibraim, E., Peccin da Silva, A., & Consoli, N.C. (2018). Modelling tensile/compressive strength ratio of artificially cemented clean sand. *Soil and Foundation*, 58(1), 199-211. https://doi.org/10.1016/j.sandf.2017.11.011.

Ferrazzo, S.T., Araújo, M.T., Bruschi, G.J., Chaves, H.M., Korf, E.P., & Consoli, N.C. (2023). Mechanical and environmental behavior of waste foundry sand stabilized with alkali-activated sugar cane bagasse ash-eggshell lime binder. *Construction & Building Materials*, 383, 131313. https://doi.org/10.1016/j.conbuildmat.2023.131313.

Farenzena, H.P., Bruschi, G.J., Schmitt Medina, G., Sousa Silva, J.P., Lotero, A., & Consoli, N.C. (2024). Iron ore tailings stabilization with alternative alkali-activated cement for dry stacking: mechanical and microstructural insights. *Canadian Geotechnical Journal*, 61(4), 649-667. https://doi.org/10.1139/cgj-2023-0125.

Ghosh, I., Guha, S., Balasubramaniam, R., & Kumar, A.V.R. (2011). Leaching of metals from fresh and sintered red mud. *Journal of Hazardous Materials*, 185(2-3), 662-668. https://doi.org/10.1016/j.jhazmat.2010.09.069.

Gonçalves, R.R.S.M., Rezende Dutra, M., Hoch, B.Z., Scheuermann Filho, H.C., Schnaid, F., & Festugato,

L. (2024). On the behavior of bauxite tailings under a wide range of stresses. *Mining*, 4(3), 629. https://doi.org/10.3390/mining4030035.

Hansen, R.N. (2015). Contaminant leaching from gold mining tailings dams in the Witwatersrand Basin, South Africa: a new geochemical modelling approach. *Applied Geochemistry*, 61, 217-223. https://doi.org/10.1016/j.apgeochem.2015.06.001.

James, L.A. (2018). Ten conceptual models of large-scale legacy sedimentation: a review. *Geomorphology*, 317, 199-217. https://doi.org/10.1016/j.geomorph.2018.05.021.

Khoeurn, K., Sakaguchi, A., Tomiyama, S., & Igarashi, T. (2019). Long-term acid generation and heavy metal leaching from the tailings of Shimokawa mine, Hokkaido, Japan: column study under natural condition. *Journal of Geochemical Exploration*, 201, 1-12. https://doi.org/10.1016/j.gexplo.2019.03.003.

Levandoski, W.M.K., Ferrazzo, S.T., Piovesan, M.A., Bruschi, G.J., Consoli, N.C., & Korf, E.P. (2024). Long-term performance: strength and metal encapsulation in alkali-activated iron ore tailings. *Environmental Science and Pollution Research International*, 31(34), 47071-47083. https://doi.org/10.1007/s11356-024-34234-5.

Liu, H., Probst, A., & Liao, B. (2005). Metal contamination of soils and crops affected by the Chenzhou lead/zinc mine spill (Hunan, China). *The Science of the Total Environment*, 339(1-3), 153-166. https://doi.org/10.1016/j.scitotenv.2004.07.030.

Mahedi, M., & Cetin, B. (2019). Leaching of elements from cement activated fly ash and slag amended soils. *Chemosphere*, 235, 565-574. https://doi.org/10.1016/j.chemosphere.2019.06.178.

Mileusnić, M., Mapani, B.S., Kamona, A.F., Ružičić, S., Mapaure, I., & Chimwamurombe, P.M. (2014). Assessment of agricultural soil contamination by potentially toxic metals dispersed from improperly disposed tailings, Kombat mine, Namibia. *Journal of Geochemical Exploration*, 144, 409-420. https://doi.org/10.1016/j.gexplo.2014.01.009.

Mitchell, J.K. (1981). Soil improvement-state of the art report. In *Proceedings of the 11th International Conference on SMFE* (Vol. 4, pp. 509-565). National Institute of Informatics. Retrieved in April 15, 2025, from https://cir.nii.ac.jp/crid/1571698599501822848

Morais, M., Levandoski, W.M.K., Reis, J.B., Rosa, F.D., & Korf, E.P. (2023). Environmental and technical feasibility of a waste foundry sand applied to pavement granular layers. *Soils and Rocks*, 46(1), e2023001722. https://doi.org/10.28927/SR.2023.001722.

Newson, T., Dyer, T., Adam, C., & Sharp, S. (2006). Effect of structure on the geotechnical properties of bauxite residue. *Journal of Geotechnical and Geoenvironmental Engineering*, 132(2), 143-151. https://doi.org/10.1061/(ASCE)1090-0241(2006)132:2(143).

Päivärinta-Antikainen, S., Huovinen, M., Ojala, S., Matějová, L., Keiski, R.L., & Vähäkangas, K.H. (2023). Leaching of metals from red mud and toxicity in human cells in vitro. *Chemosphere*, 332, 138807. https://doi.org/10.1016/j.chemosphere.2023.138807.

Rissoli, A.L.C., Pereira, G.S., Mendes, A.J.C., Scheuermann Filho, H.C., Carvalho, J.V.D.A., Wagner, A.C., Silva, J.P.D.S., & Consoli, N.C. (2024). Dry stacking of filtered iron ore tailings: comparing on-field performance of two drying methods. *Geotechnical and Geological Engineering*, 42(4), 2937-2948. https://doi.org/10.1007/s10706-023-02689-x.

Sandroni, S.S., & Guidicini, G. (2022). *Barragens de terra e enrocamento*. São Paulo: Oficina de Textos.

Santos, C.P.D., Bruschi, G.J., Tonatto Ferrazzo, S., Kubiaki Levandoski, W.M., Pavan Korf, E., & Consoli, N.C. (2025). Leaching behavior of alkali-activated gold tailings over wetting–drying cycles. *Indian Geotechnical Journal*, 55(1), 176-190. https://doi.org/10.1007/s40098-024-00886-w.

Saraiva, R.D.S., Santos, A.S.E., Oliveira, A.P.N., Mazoto, M.L., Câmara, V.M., & Asmus, C.I.F.R. (2024). Alterações respiratórias em crianças expostas à poeira de resíduos de mineração em Brumadinho, Minas Gerais, Brasil: projeto Bruminha. *Cadernos de Saúde Pública*, 40(2), e00131223. https://doi.org/10.1590/0102-311xpt131223.

Scheuermann Filho, H.C., & Consoli, N.C. (2024). Effect of porosity/cement index on behavior of a cemented soil: the role of dosage change. *Geotechnical and Geological Engineering*, 42(1), 351-368. https://doi.org/10.1007/s10706-023-02577-4.

Schnaid, F., Prietto, P.D.M., & Consoli, N.C. (2001). Characterization of cemented sand in triaxial compression. *Journal of Geotechnical and Geoenvironmental Engineering*, 127(10), 857-868. https://doi.org/10.1061/(ASCE)1090-0241(2001)127:10(857).

Servi, S., Lotero, A., Silva, J.P.S., Bastos, C., & Consoli, N.C. (2022). Mechanical response of filtered and compacted iron ore tailings with different cementing agents: focus on tailings-binder mixtures disposal by stacking. *Construction & Building Materials*, 349, 128770. https://doi.org/10.1016/j.conbuildmat.2022.128770.

Stracke, F., Jung, J.G., Korf, E.P., & Consoli, N.C. (2012). The influence of moisture content on tensile and compressive strength of artificially cemented sand. *Soils and Rocks*, 35(3), 303-308. https://doi.org/10.28927/SR.353303.

Tang, L., He, Z., Chen, K., Wang, X., Xiao, Y., Yu, Z., & Xiao, H. (2023). Study of microscopic properties and heavy metal solidification mechanism of electrolytic manganese residue-based cementitious materials. *Environmental Science and Pollution Research International*, 30(48), 105056-105071. https://doi.org/10.1007/s11356-023-29772-3.

Tian, H., Williams, D.J., Mandisodza, K., Zhang, C., Olaya, S.Q., Zhang, W., & Tang, C. (2023). Engineering properties of fine-grained red mud. *International Journal of Mining, Reclamation and Environment*, 37(6), 399-418. https://doi.org/10.1080/17480930.2023.2212575.

U.S. Environmental Protection Agency – USEPA. (2025). *Ground water and drinking water: national primary drinking water regulations.* Retrieved in April 15, 2025, from https:// www.epa.gov/ground-water-and-drinking-water/national-primary-drinking-water-regulations#Inorganic

Wagner, A.C., Sousa Silva, J.P., Azambuja Carvalho, J.V., Cezar Rissoli, A.L., Cacciari, P.P., Chaves, H.M., Scheuermann Filho, H.C., & Consoli, N.C. (2023). Mechanical behavior of iron ore tailings under standard compression and extension triaxial stress paths. *Journal of Rock Mechanics and Geotechnical Engineering*, 15(7), 1883-1894. https://doi.org/10.1016/j.jrmge.2022.11.013.

Wang, F., Long, G., Bai, M., Wang, J., Zhou, J.L., & Zhou, X. (2022). Application of electrolytic manganese residues in cement products through pozzolanic activity motivation and calcination. *Journal of Cleaner Production*, 338, 130629. https://doi.org/10.1016/j.jclepro.2022.130629.

Wang, D., Wang, Q., Cui, Y., & Pang, L. (2023). Assessing heavy-metal leaching risk in cement-industrial slag composite pastes using a mechanism-based thermodynamic approach. *Cement and Concrete Composites*, 140, 105074. https://doi.org/10.1016/j.cemconcomp.2023.105074.

Williams, D.J. (2021). Lessons from tailings dam failures: where to go from here? *Minerals* , 11(8), 853. https:// doi.org/10.3390/min11080853.